Thermochimica Acta, 147 (1989) 361–375
Elsevier Science Publishers B.V., Amsterdam – Printed in The Netherlands

XPS AND TPD PROBE TECHNIQUES FOR THE STUDY OF $LaNiO_3$ PEROVSKITE OXIDE

LUIS G. TEJUCA * and JOSÉ LUIS G. FIERRO **
Instituto de Catálisis y Petroleoquímica, C.S.I.C., Serrano 119, 28006 Madrid (Spain)
(Received 12 December 1988)

ABSTRACT

The surface of $LaNiO_3$ and the interactions of CO, CO_2 and hydrogen with this perovskite were studied as a function of the reduction temperature of the oxide. The evolution of the oxygen and lanthanum X-ray photoelectron spectroscopy (XPS) photolines is consistent with the formation and decomposition of an oxyhydroxide LaO(OH) species. CO adsorption yields CO temperature-programmed desorption (TPD) peaks at 365–385 K (assigned to CO linearly bonded to Ni^{2+}) and 745–930 K (assigned to bridged CO on Ni^0 centres) and CO_2 peaks at 500 K and above (assigned to surface carbonates). CO_2 adsorption yields CO_2 TPD peaks at 340–375 K and above 600 K which are assigned to monodentate and bidentate or bridged carbonates respectively. There are no significant differences between the hydrogen and CO TPD spectra obtained after $CO–H_2$ and $H_2–CO$ adsorption sequences and after the adsorption of CO or hydrogen on $LaNiO_3$ reduced at 773 K. These results indicate that no interaction (or a weak interaction) occurs between CO and hydrogen in the adsorbed state. This is in contrast with adsorption results on $LaCrO_3$ reduced at 923 K. This different behaviour appears to be related to the relative strengths of the interactions of CO and hydrogen with the surfaces of these reduced oxides.

INTRODUCTION

The bulk and surface properties of $LaNiO_3$ have been studied by several workers. Wachowski et al. [1] obtained a slightly oxygen-deficient perovskite $LaNiO_{2.98}$ using the explosion method. X-ray photoelectron spectroscopy (XPS) measurements showed that the reductive non-stoichiometry at the surface was much more pronounced than that found in the bulk [2]. This perovskite has a rather low metal–oxygen binding energy (approximately 313 kJ mol^{-1}) [3] and is susceptible to reduction in hydrogen to one electron per molecule at 600 K and three electrons per molecule at 750 K (at a programmed heating rate of 4 K min^{-1}) [4]. Crespin et al. [5] using a slower heating rate (0.08 K min^{-1}) found reduction steps of one, two and three electrons per molecule at 573, 643 and 728 K respectively. $La_2Ni_2O_5$ and

* Deceased.
** To whom all correspondence should be addressed.

0040-6031/89/$03.50

$LaNiO_2$ were identified as intermediate reduced phases by X-ray diffraction and extended X-ray absorption fine structure (EXAFS) [5,6]. Both compounds are stable in air at room temperature. However, after heating in helium at 1273 K a dismutation reaction occurs with the formation of La_2NiO_4, NiO and nickel. La_2NiO_4, with the K_2NiF_4 structure has also been found by Nakamura et al. [7] in the reduction of $LaNiO_3$ at 1273 K. NO adsorption on $LaNiO_3$ has been studied by Tascón et al. [8]. Hydrogen, C_2H_6 and C_2H_4 adsorption on $La_2Ni_2O_5$ has been studied by Crespin et al. [9]. This phase with the brownmillerite structure is active for ethylene hydrogenation. $LaNiO_3$ has also been found to be active for CO and hydrocarbon oxidation [10,11], homomolecular exchange of oxygen [12], N_2O decomposition [13] and 2-propanol dehydrogenation and dehydration [14].

CO hydrogenation is of particular interest to obtain oxygenated organic compounds. Supported noble metals have been used for these reactions [15,16]. However, perovskite oxides have also been found to be catalytically active [17–21]. Thus, Broussard and Wade [20] found selectivities of over 20% for alcohol synthesis on $LaNiO_3$. Nickel in the bulk of the catalyst was found to be Ni^+ and Ni^0. No data were given for its oxidation state at the surface. In this work the surface of $LaNiO_3$ and the interactions of CO, CO_2 and hydrogen with this perovskite (at different degrees of reduction) were studied using XPS and temperature-programmed desorption (TPD). This information should be of interest in understanding the catalytic behaviour of $LaNiO_3$ for CO hydrogenation.

EXPERIMENTAL

Materials

$LaNiO_3$ was prepared using the amorphous citrate method as described previously [22]. The decomposition of the precursor was carried out using the conditions previously determined (at 1023 K for 4 h in air) to obtain a single perovskite phase. The BET specific surface area of the sample, as determined by nitrogen adsorption at 77 K, was 5.8 $m^2\ g^{-1}$. The gases used (helium, hydrogen, CO and CO_2) and a 21%O_2–79%He mixture were purified by standard methods. The high purity helium (99.998%) used as carrier in the TPD runs was further purged of its main impurity (oxygen) down to less than 1 ppm.

Equipment and methods

X-ray photoelectron spectra were acquired with a Leybold Heraeus LHS10 electron spectrometer equipped with a hemispherical analyser and a magnesium anode ($h\nu$ = 1253.6 eV) as excitation source. The energy scale of the

instrument was calibrated taking the C 1s line at 284.6 eV as reference. Spectra were taken for oxidized (as-prepared), outgassed (as-specified) and reduced (in a hydrogen flow for 2 h at the desired temperature) samples (sample notation as for TPD, see below). After outgassing or reduction the sample was cooled to room temperature in a helium stream and mounted on a long rod for introduction into the spectrometer chamber where it was outgassed at approximately 10^{-5} Torr (1 Torr = 133.3 N m^{-2}) for 0.5 h at room temperature. It was then introduced into the analysis chamber where the pressure was maintained below 7×10^{-9} Torr during data acquisition. Energy regions (20-eV) of the photoelectrons of interest were recorded using an on-line computer at 20 eV pass energy on the analyser. Only photolines for the O 1s and La 4d levels are given. Ni 2p photolines were not recorded because the most intense peak of the 2p doublet (Ni $2p_{3/2}$) overlaps with the La $3d_{3/2}$ peak at binding energies near 855 eV.

The $LaNiO_3$ sample (0.5 g) used in the TPD runs was placed in a quartz reactor which could be heated at variable programmed temperatures up to 1 K s^{-1}. The analysis of the effluent gases was performed with a UTI model 100C mass spectrometer. TPD experiments were performed after gas adsorption on oxidized and reduced samples. For oxidation the 21%O_2–79% He mixture was passed through the sample for 1 h at 923 K. Reduced samples were prepared from oxidized $LaNiO_3$ by passing a hydrogen flow for 1 h at the desired temperature. The samples so treated are referred to as $LaNiO_3$ (ox 923) and $LaNiO_3$ (red T) where T is the reduction temperature in Kelvin. After the appropriate oxidation or reduction treatments the sample was outgassed by passing a helium flow through the reactor for 1 h at 923 K. The adsorption of individual gases was effected by passing a flow of CO, CO_2 or hydrogen for 0.5 h at 298 K followed by a helium flow for 15 min at 298 K to remove the physisorbed part. The successive CO–H_2 adsorption was carried out by passing flows of CO (0.5 h, 298 K), helium (15 min, 298 K), hydrogen (0.5 h, 298 K) and helium (15 min, 298 K). H_2–CO adsorption was carried out as above passing hydrogen first and then CO. After the oxidation, reduction, outgassing and adsorption steps, the reactor was repressurized with helium. Heating of the catalyst bed was then started at 0.5 K min^{-1}. The maximum heating temperature was limited to 923 K (100 K below the preparation temperature). Between successive TPD runs the sample underwent treatments of oxidation, reduction and outgassing as above. A flow rate of 50 cm^3 min^{-1} was used for all steps. Temperatures for peak maxima in TPD spectra are indicated by T_{max}.

RESULTS AND DISCUSSION

X-ray photoelectron spectroscopy

X-ray photoelectron spectra of the O 1s and La 4d photoemission levels of as-prepared $LaNiO_3$ and of samples after outgassing and reduction

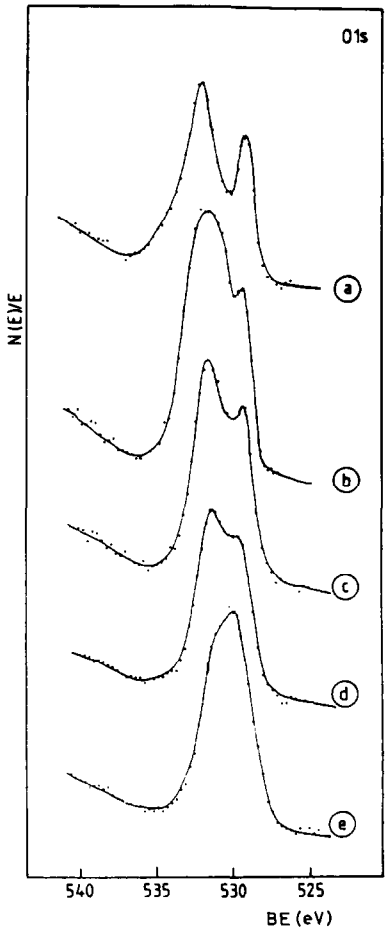

Fig. 1. O 1s core level spectra of as-prepared $LaNiO_3$ (a), after outgassing under high vacuum for 2 h at 723 K (b) and after reduction in hydrogen at 473 K (c), 573 K (d) and 673 K (e).

treatments are given in Figs. 1 and 2. The corresponding binding energies (BE) are collected in Table 1. The O 1s spectra (Fig. 1) present two maxima at 528.2–529.6 eV and at 530.7–530.9 eV. In addition, the peak at higher BE of the as-prepared sample (Fig. 1(a)) shows an asymmetry towards higher BEs which disappears for the outgassed (Fig. 1(b)) and reduced (Figs. 1(c)–1(e)) samples. The relative intensity of the peak at higher BE undergoes a remarkable decrease for samples reduced at 473–673 K (Figs. 1(c)–1(e)). The photoline at lower BE is assigned to lattice oxygen O^{2-}. That at higher BE is assigned to less electron-rich species of oxygen in the adsorbed state such as OH^- [2,23–28] although, in some instances, absorbed oxygen has been assumed to be associated with this photoline [24]. It should be noted that the hydrogen atom is not detectable by XPS because of its exceptionally low photoionization cross-section. The presence of other species with a net

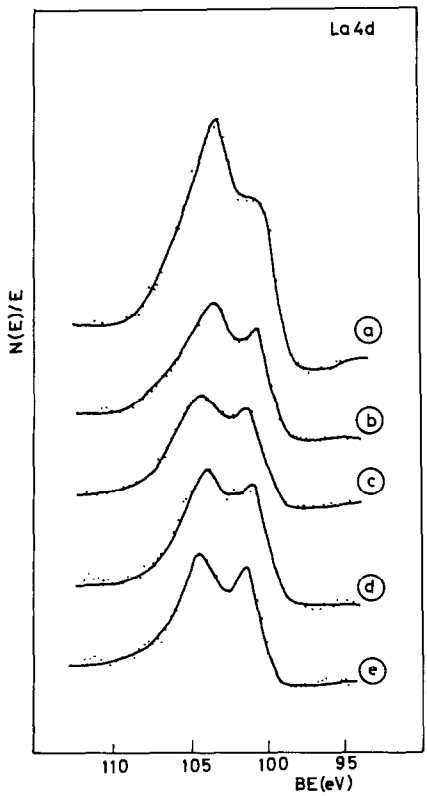

Fig. 2. La 4d core level spectra of $LaNiO_3$ samples as in Fig. 1.

charge of unity such as O^- or O_2^{2-} is extremely unlikely given their high reactivity and the observed decrease in intensity of the photoline at higher BE with increasing reduction temperature. The asymmetry of the peak at higher BE in Fig. 1(a) corresponds to adsorbed molecular water which is not removed during conditioning of the sample (outgassing at room temperature) in the ultrahigh vacuum chamber.

TABLE 1

Binding energies [a] (eV) of electrons for O 1s and La $4d_{5/2}$ atomic levels and relative intensity ratios of La 4d electrons

Sample pretreatment	O 1s	La $4d_{5/2}$	$I(\text{La } 4d_{3/2})/I(\text{La } 4d_{5/2})$
As-prepared	530.9–528.2	100.7	1.45
Outgassing at 723 K	530.7–528.8	100.6	1.16
Reduction in H_2, 473 K	530.8–529.1	101.4	1.15
Reduction in H_2, 573 K	530.9–529.0	101.0	1.14
Reduction in H_2, 673 K	530.8–529.6	101.3	1.05

[a] Referenced to the C 1s photoline at 284.6 eV.

Substantial changes are also observed for the La 4d photolines (Fig. 2, Table 1). Thus, the ratio of the intensities of the La $4d_{3/2}$ and La $4d_{5/2}$ levels decreases markedly with increasing reduction temperature. Its value after reduction at 673 K is very close to that expected for La_2O_3. It should be noted that this decrease runs parallel with the decrease in the relative intensity observed for the O 1s peak at higher BE. These results are consistent with the formation of an oxyhydroxide LaO(OH) in the unreduced sample and its gradual decomposition after reduction according to the reaction

$$2LaO(OH) \rightarrow La_2O_3 + H_2O \quad (1)$$

This behaviour, for samples reduced in dynamic conditions, is opposite to that observed for $LaCoO_3$ reduced in static conditions [27]. In the latter case the intensity of the O 1s peak at higher BE increases for increasing reduction temperature because the presence of the water produced in the reduction process (eqn. (1)) displaces the equilibrium towards formation of LaO(OH).

Temperature-programmed desorption spectroscopy

CO adsorption

Temperature-programmed desorption spectra of CO after CO adsorption at 298 K on $LaNiO_3$ reduced at increasing temperatures are given in Fig. 3. These include a peak at 365–385 K whose intensity is at a maximum for $LaNiO_3$ (red 673) and then decreases for $LaNiO_3$ (red 773). The intensity change suggests that this peak is associated with CO interacting with an intermediate oxidation state of nickel. Previous experiments of temperature-programmed reduction in hydrogen and X-ray diffraction have shown that $LaNiO_3$ reduces to one electron per molecule at 600 K and to three electrons per molecule at 750 K [4]. This is shown in Table 2 where reduction temperatures and reduction degrees are given for several perovskites [4,29–32]. Therefore, this TPD peak should be associated with CO bonded to Ni^{2+}. Other TPD peaks appearing between 745 and 930 K, whose intensities increase with the reduction temperature of the oxide, should be due to CO species of a higher thermal stability interacting with Ni^0 centres. Metallic nickel has been detected by X-ray diffraction after reduction of $LaNiO_3$ below one electron per molecule (in hydrogen at 515 K) and heating in helium at 1073 K [4]. Before the sintering process in helium no peaks of Ni^0 are detected, indicating that metallic nickel is present, after gentle reduction, in a highly dispersed state.

After CO adsorption at room temperature on reduced Ni–SiO_2 samples, Blackmond and Ko [33] found IR bands at 2080 ad 2040 cm^{-1} of sub-carbonyl or linearly bonded species. An additional broad band at 1950 cm^{-1} showing contributions from more than one unresolved peak was attributed to twofold, threefold and fourfold bridged CO on different crystallographic

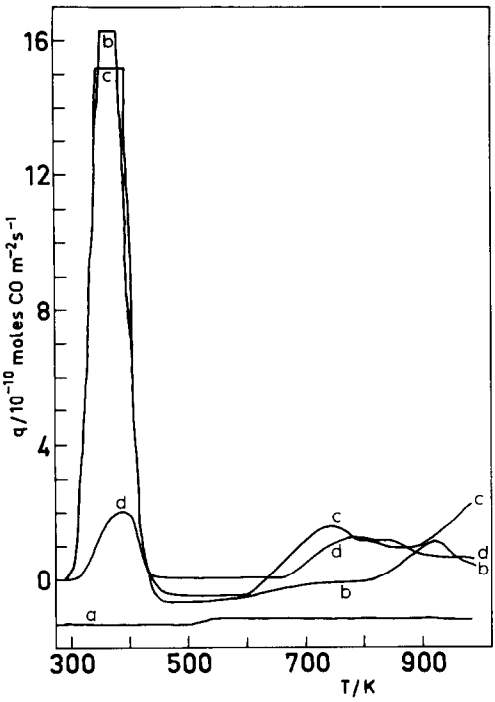

Fig. 3. TPD spectra of CO after CO adsorption at 298 K on $LaNiO_3$ reduced in hydrogen at 473 K (a), 573 K (b), 673 K (c) and 773 K (d).

planes of nickel. Therefore, the CO peak at lower desorption temperatures (365–385 K, Fig. 3) can be assigned to linear CO species interacting with Ni^{2+} and the overlapping peaks at 745–930 K can be assigned to bridged CO species adsorbed on Ni^0 centres. Blackmond and Ko [33] also observed

TABLE 2

Reduction of $LaMO_3$ oxides

Oxide	Reduction temperature (K)	Reduction degree (electrons per molecule)	Reference
$LaCrO_3$ [a]	1270	1.3×10^{-2}	29
$LaMnO_3$ [a]	1173	1	30
$LaFeO_3$ [a]	1173	3	31
$LaCoO_3$ [b]	723	1	32
	898	3	
$LaNiO_3$ [a]	600	1	4
	748	3	

[a] From temperature-programmed reduction in 300 Torr H_2 (static system). Heating rate, 4 K min^{-1}.

[b] From temperature-programmed reduction in D_2 (recirculating system). Heating rate, 3 K min^{-1}.

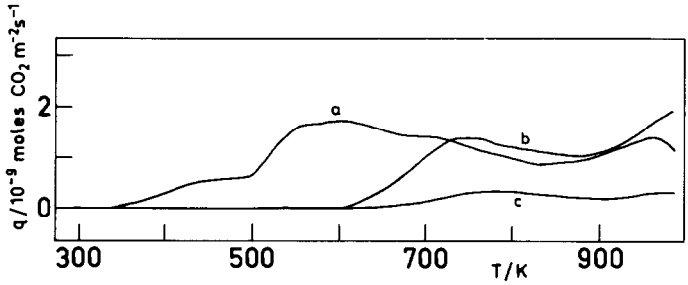

Fig. 4. TPD spectra of CO_2 after CO adsorption at 298 K on $LaNiO_3$ reduced in hydrogen at 473 K (a), 673 K (b) and 773 K (c).

an increase in the relative concentration of bridged species for increasing reduction temperature since the ratio $CO_{ads} : H_{ads}$ decreased in that direction. On the other hand, Raupp and Dumesic [34] found a slight increase in the strength of CO adsorption on TiO_2 with increasing extent of surface reduction. These results are certainly in agreement with those in Fig. 3 which show a decrease and an increase in intensity respectively, for the peaks attributed to linear and bridged CO, with increasing reduction temperature.

CO adsorption on $LaNiO_3$ (red 473) also yields CO_2 TPD peaks at 505, 695 and 960 K which shift to higher desorption temperatures with increasing degree of reduction of the perovskite (Fig. 4). Their intensities decrease as the availability of surface O^{2-} decreases, i.e. for increasing reduction temperature. Therefore, the desorbed CO_2 should be due to interaction of CO with lattice oxygen and subsequent formation and decomposition of surface carbonates.

CO_2 adsorption

Temperature-programmed desorption spectra of CO_2 obtained after CO_2 adsorption at 298 K on reduced $LaNiO_3$ are given in Fig. 5. They are rather complex and are composed of peaks at 340–375 K, 600–665 K, 710–750 K and 875–970 K; they are assigned to decomposition of carbonates of different thermal stabilities: monodentate (peaks at 340–375 K) and bidentate or bridged (peaks above 600 K) carbonates. No information has been obtained from IR spectroscopy because of the low transmittance of this perovskite. However, the presence of these species has been reported after CO_2 adsorption on other simple oxides and perovskites [34–36]. The peaks appearing above 600 K present intensity maxima for $LaNiO_3$ (red 573). This effect is similar to that observed for the CO desorption peak (after CO adsorption) appearing at 365–385 K (Fig. 3) and suggests that these carbonates are associated with Ni^{2+}. The bridged carbonates interact with two metal cations; these should be Ni^{2+} and La^{3+} given the strong basic character of the latter cation and the acidic character of the CO_2 molecule. Interaction with La^{3+} is supported by the fact that the observed CO_2

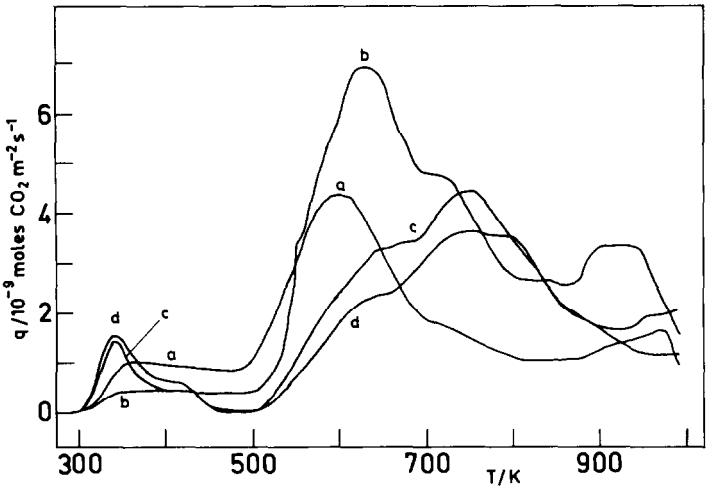

Fig. 5. TPD spectra of CO_2 after CO_2 adsorption at 298 K on $LaNiO_3$ reduced in hydrogen at 473 K (a), 573 K (b), 673 K (c) and 773 K (d).

desorption after CO_2 adsorption is higher than the $CO + CO_2$ desorption after CO adsorption.

CO and H_2 successive adsorption

The TPD spectra of hydrogen after $CO–H_2$ and $H_2–CO$ adsorption sequences at 298 K on $LaNiO_3$ (red 773) are given in Fig. 6. They show similar profiles and do not present significant differences with respect to that obtained after adsorption of hydrogen only. Values of T_{max} for these spectra are given in Table 3. Similar values are found regardless of the adsorption mode considered. Spinicci and Tofanari [37] have found TPD peaks of hydrogen (after adsorption of hydrogen on $Ni–SiO_2$ at room

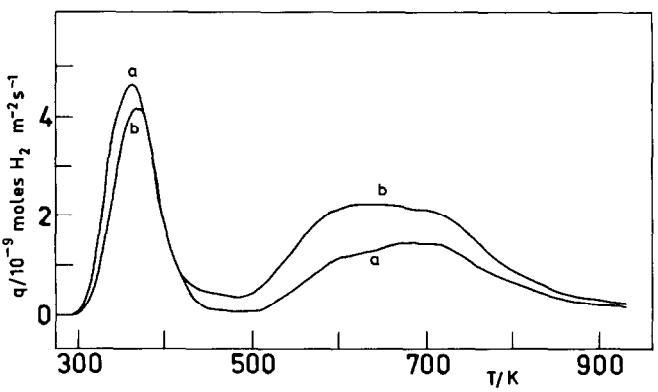

Fig. 6. TPD spectra of hydrogen after $CO–H_2$ (a) and $H_2–CO$ (b) successive adsorption at 298 K on $LaNiO_3$ reduced in hydrogen at 773 K.

TABLE 3

Temperature of hydrogen and CO desorption peaks (T_{max}) after hydrogen or CO adsorption only and after CO–H_2 and H_2–CO sequential adsorption at 298 K on $LaNiO_3$ reduced in hydrogen at 773 K

Adsorption sequence	T_{max} (K)	
	H_2	CO
H_2 or CO adsorption only	350, 615, 685	385, 795, 925
CO–H_2	355, 625, 685	385, 815, 870
H_2–CO	365, 640, 695	360, 790, 875

temperature) with desorption maxima (at approximately 355 and 595 K) very similar to those found in this work (Table 3). However, Rynkowski [38] reported TPD peaks of hydrogen adsorbed on Ni–Al_2O_3 at higher desorption temperatures (approximately 450 and 900 K).

It has been found [39] that hydrogen adsorption on $LaNiO_3$ (reduced in the temperature zone 473–773 K) yields TPD spectra of hydrogen composed of one peak at a T_{max} value of 340–355 K and a broad peak (overlapping peaks) at a T_{max} value of 610 K and above (these latter peaks appear only for reduction temperatures equal to or higher than 573 K). The intensities of these peaks increase with increasing reduction temperature suggesting that they are associated with hydrogen adsorption on reduced metallic sites since nickel in $LaNiO_3$ (red 773) should be Ni^0 (see Table 2). Likewise, Kuijpers et al. [40,41] have found hydrogen adsorption at 300 K on reduced Ni–SiO_2 catalysts and have shown that hydrogen does not adsorb at 300 K on oxidized NiO. Therefore, the TPD peaks in Fig. 6 can be assigned to hydrogen adsorbed on Ni^0.

As for hydrogen, no substantial differences are found in the CO desorption spectra after CO–H_2 and H_2–CO adsorption sequences and after CO adsorpion only (Figs. 3(d) and 7; Table 3). These results indicate that no interaction (or a weak interaction) occurs between CO and hydrogen in the adsorbed state. In agreement with this finding, Prinsloo and Gravelle [42] have demonstrated, using calorimetric studies, that there is no chemical

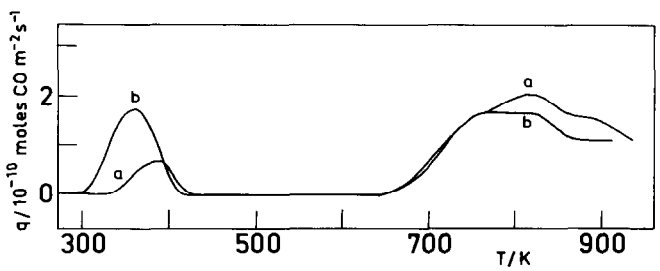

Fig. 7. TPD spectra of CO after CO–H_2 (a) and H_2–CO (b) successive adsorption at 298 K on $LaNiO_3$ reduced in hydrogen at 773 K.

interaction between CO and hydrogen in a mixed adsorbate layer containing these molecules at 296 K on reduced Ni–SiO_2, i.e. no new surface complex or product appears. Similar results have been found by Gopalakrishnan and Viswanathan [43] on a polycrystalline cobalt surface at room temperature.

Comparative behaviour of $LaMO_3$ oxides

From the results obtained after adsorption of hydrogen, CO and CO_2 at 298 K on reduced (in a hydrogen flow of 50 cm^3 min^{-1}) $LaMO_3$ (M = Cr, Mn, Fe, Co, Ni) [27,44,45], some general features of the interaction of these probe molecules with the adsorbent surface can be described. The spectra were studied as a function of the reduction temperature of the oxide.

After CO_2 adsorption at 298 K on $LaMnO_3$ reduced at 723–873 K [45], on $LaCrO_3$ reduced at 623–923 K and on $LaFeO_3$ reduced at 823 K [44], peaks of CO (in addition to peaks of CO_2) desorption are observed. These are due to CO_2 reduction on the reduced surface of the oxide. However, no CO desorption peaks are observed after CO_2 adsorption on $LaCoO_3$ (red 773) [27] and $LaNiO_3$ (red 773) (Fig. 5). This may be related to the higher catalytic activity for CO oxidation of $LaCoO_3$ and $LaNiO_3$ with respect to the activity of the rest of the $LaMO_3$ series of oxides [10].

CO_2 adsorption on the less reducible oxides of the series, namely $LaMnO_3$ [45], $LaCrO_3$ and $LaFeO_3$ [44] yields two main TPD peaks of CO_2 at 340–390 K and 540–970 K. Those appearing at the higher desorption temperatures increase in intensity with increasing reduction temperature of the oxide. This is interpreted to indicate formation and decomposition of bidentate or bridged carbonates interacting with one or two metal cations. The presence of these species is confirmed by IR spectroscopy. Formation of this type of carbonate from CO_2 takes place on surface sites composed of a lattice oxygen and an anion vacancy (O^{2-} □) (□, anion vacancy) [46]. Consistent with this interpretation, the concentrations of these carbonate species increase with increasing concentration of the above surface sites, i.e. with increasing degree of reduction of the oxide. It is worth noting that this effect (increase in the TPD peak appearing at higher desorption temperatures) is less notorious on reduced $LaCrO_3$ (the member of the $LaMO_3$ series which is most difficult to reduce (see Table 2) and more evident on reduced $LaMnO_3$ and $LaFeO_3$.

The evolution of the corresponding TPD peaks obtained after CO_2 adsorption on reduced $LaCoO_3$ [27] and $LaNiO_3$ (Fig. 5) (the most easily reducible oxides, Table 2) is very different. In both cases, the intensities of the TPD peaks show maxima for samples reduced at 573 K and decrease for higher reduction temperatures. These results indicate interaction of bidentate or bridged carbonates with intermediate reduction states of cobalt and nickel, namely Co^{2+} and Ni^{2+}. Indeed, experiments of temperature-programmed reduction in hydrogen or deuterium of the $LaMO_3$ oxides up to approximately 1200 K show that only $LaCoO_3$ and $LaNiO_3$ present a stable

intermediate reduction state of one electron per molecule (Table 2). $LaCrO_3$ does not show any significant reduction in this temperature range. $LaMnO_3$ reduces only to one electron per molecule and $LaFeO_3$ reduces directly to three electrons per molecule. Therefore it is assumed that an important factor in the formation of these carbonates from CO_2 adsorption on reduced $LaCoO_3$ and $LaNiO_3$ is the availability of Co^{2+} and Ni^{2+}. The number of pair sites needed for adsorption (O^{2-} □) appears to increase in these latter oxides up to a reduction temperature of 573 K, where the reduction degree and the concentration of anion vacancies may be expected to increase moderately. At higher reduction temperatures the concentration of anion vacancies will increase drastically thus decreasing the concentration of pair sites and, therefore, hindering the formation of bidentate or bridged carbonates. It should be noted that the temperature for attaining a given reduction degree in TPD experiments (isothermal heating in flowing hydrogen for 1 h) is lower than that indicated by temperature-programmed reduction.

The different $LaMO_3$ oxides yield substantially different interactions with CO and hydrogen [27,44,45]. These differences are more conspicuous between the extremes of the series. Hydrogen, CO and CO_2 TPD spectra obtained after CO–H_2 sequential adsorption at 298 K on $LaCrO_3$ reduced in hydrogen at 923 K are very different from the TPD spectra obtained after the adsorption of hydrogen or CO only [44]. These differences refer to the amounts of gas desorbed and to the temperatures of the peak maxima and are assumed to be due to strong interactions between CO and hydrogen in the adsorbed state with formation of an oxygenated surface species. CO pre-adsorption on this reduced oxide inhibits subsequent hydrogen adsorption more severely than hydrogen pre-adsorption inhibits subsequent CO adsorption. This is taken to be indicative of CO interacting more strongly than hydrogen with $LaCrO_3$ (red 923). It appears that this stronger interaction Cr^{n+}–CO ($n < 3$) favours the mutual interaction CO–hydrogen. The reverse adsorption sequence H_2–CO does not give rise to any strong interaction between adsorbed CO and hydrogen since no substantial differences in hydrogen, CO and CO_2 TPD spectra are observed with respect to those obtained after the adsorption of hydrogen or CO only. In this study no significant differences are observed in the hydrogen and CO TPD spectra obtained after CO–H_2 or H_2–CO sequences and after the adsorption of hydrogen or CO only on $LaNiO_3$ (red 773) (Figs. 6 and 7). These results indicate that no interaction (or a weak interaction) occurs, in this case, between adsorbed CO and hydrogen (see above).

TPD spectra of hydrogen, after hydrogen adsorption on $LaCrO_3$ reduced at variable temperatures (523–923 K), show only one peak whose T_{max} is practically constant (375–395 K) and whose intensity increases with the reduction temperature of the perovskite [39]. These results show that hydrogen adsorbs on reduced Cr^{n+} ($n < 3$) and that the strength of the adsorption

bond of hydrogen with the adsorbent surface does not change in any significant way with the reduction temperature. However, results of hydrogen adsorption on reduced $LaNiO_3$ [39] (see above) show that a substantial fraction of adsorbed hydrogen (desorption peaks at $T_{max} \geqslant 610$ K) interacts with the surface of $LaNiO_3$ (red 773) much more strongly than with the surface of $LaCrO_3$ (red 923). This stronger adsorption bond of hydrogen may hinder its interaction with CO adsorbed on $LaNiO_3$ (red 773) and impede the subsequent formation of an oxygenated species at the surface of this reduced perovskite. Thus, the different behaviours of reduced $LaCrO_3$ and reduced $LaNiO_3$ seem to be related to the relative strengths of the interactions of CO and hydrogen with the surfaces of these materials. These results may be indicative of important differences in the catalytic behaviour of $LaCrO_3$ and $LaNiO_3$ for $CO + H_2$ reaction since the above species may be intermediate in the formation of oxygenated organic compounds. As far as we know there are no catalytic data available which would allow us to shed light on a possible relationship between the strength of the CO and hydrogen adsorption bonds on these reduced perovskites and their hydrogenation activity.

CONCLUSIONS

The surface of $LaNiO_3$ and the interactions of CO, CO_2 and hydrogen with this perovskite as a function of the reduction (in dynamic conditions) temperature of the oxide were studied using XPS and TPD spectroscopies. The following conclusions may be drawn.

The XPS spectra of the O 1s levels present maxima at 528.2–529.6 eV due to lattice oxygen and at 530.7–530.9 eV due to hydroxyl groups. The intensity of the latter photoline and the intensity ratio La $4d_{3/2}$/La $4d_{5/2}$ decrease markedly with increasing reduction temperature. These results are consistent with the formation of the oxyhydroxide LaO(OH) in the unreduced sample and its gradual decomposition into La_2O_3 and water.

TPD spectra of CO after CO adsorption at 298 K on reduced $LaNiO_3$ include peaks at 365–385 K (due to linearly adsorbed CO on Ni^{2+} centres) and 745–930 K (due to bridged CO species on Ni^0 centres). CO adsorption also yields overlapping peaks of CO_2 at 500 K and above which are assigned to surface carbonates.

CO_2 adsorption yields CO_2 TPD peaks at 340–375 K (monodentate carbonates) and above 600 K (bidentate or bridged carbonates). The latter peaks show intensity maxima for $LaNiO_3$ reduced at 573 K, suggesting that these carbonates are associated with Ni^{2+}.

The TPD spectra of hydrogen after the adsorption sequences $CO–H_2$ and $H_2–CO$ on $LaNiO_3$ (red 773) (with peaks at 350–365 K and overlapping peaks above 600 K which are assigned to hydrogen adsorbed on Ni^0 centres) do not present significant differences from those obtained after the adsorp-

tion of H_2 only. TPD spectra of CO after CO–H_2 and H_2–CO sequences are also similar to the CO spectra after adsorption of CO only. These results indicate that no interaction (or a weak interaction) occurs between CO and hydrogen in the adsorbed state.

TPD peaks of CO (in addition to peaks of CO_2) are observed after CO_2 adsorption on reduced $LaCrO_3$, $LaMnO_3$ and $LaFeO_3$. However, no CO desorption peaks are observed after CO_2 adsorption on reduced $LaCoO_3$ and $LaNiO_3$. This finding can be related to the higher catalytic activity for CO oxidation of the latter perovskites with respect to the activity of the rest of the $LaMO_3$ series.

The concentration of bidentate or bridged carbonates formed by CO_2 adsorption on pair sites (O^{2-} □) increases with increasing reduction temperature on the less reducible oxides, namely $LaCrO_3$, $LaMnO_3$ and $LaFeO_3$. However, the concentration of these carbonates formed on the more reducible oxides is at a maximum for $LaCoO_3$ (red 573) and $LaNiO_3$ (red 573) and decreases for higher reduction temperatures. The number of pair sites needed for adsorption appears to increase on these latter oxides up to a reduction temperature of 573 K where the reduction degree and the concentration of anion vacancies may be expected to increase moderately. At higher reduction temperatures the concentration of anion vacancies will increase drastically thus decreasing the concentration of pair sites and therefore hindering the formation of bidentate or bridged carbonates.

The different $LaMO_3$ oxides yield substantially different CO–hydrogen interactions in the adsorbed state; these differences are more conspicuous between the extremes of the series. Thus, a strong interaction between CO and hydrogen (after the adsorption sequence CO–H_2) with formation of an oxygenated surface species occurs on $LaCrO_3$ (red 923). However, no interaction (or a weak interaction) occurs between these molecules adsorbed on $LaNiO_3$ (red 773). This different behaviour appears to be related to the relative strengths of the interactions of CO and hydrogen with the surfaces of these reduced oxides.

ACKNOWLEDGEMENT

The authors are greatly indebted to the Spanish–North American Joint Committee for Scientific and Technological Cooperation for sponsorship of this work (Project No. CCB8409-003).

REFERENCES

1 L.Wachowski, S. Zielinski and A. Burewicz, Acta Chim. Acad. Sci. Hung., 106 (1981) 217.
2 J.L.G. Fierro and L.G. Tejuca, Appl. Surf. Sci., 27 (1987) 453.
3 T. Shimizu, Chem. Lett., (1980) 1.
4 J.L.G. Fierro, J.M.D. Tascón and L.G. Tejuca, J. Catal., 93 (1985) 83.
5 M. Crespin, P. Levitz and L. Gatineau, J. Chem. Soc., Faraday Trans. 2, 79 (1983) 1181.

6 P. Levitz, M. Crespin and L. Gatineau, J. Chem. Soc., Faraday Trans. 2, 79 (1983) 1195.
7 T. Nakamura, G. Petzow and L.J. Gauckler, Mater. Res. Bull., 14 (1979) 649.
8 J.M.D. Tascón, L.G. Tejuca and C.H. Rochester, J. Catal., 95 (1985) 558.
9 M. Crespin, L. Gatineau, J. Fripiat, H. Nijs, J. Marcos and E. Lombardo, Nouv. J. Chim., 7 (1983) 477.
10 J.M.D. Tascón and L.G. Tejuca, React. Kinet. Catal. Lett., 15 (1980) 185.
11 G. Kremenic, J.M.L. Nieto, J.M.D. Tascón and L.G. Tejuca, J. Chem. Soc., Faraday Trans. 1, 81 (1985) 939.
12 L.A. Sazonov, Z.V. Moskvina and E.V. Artamonov, Kinet. Catal., 15 (1974) 100.
13 K.V. Ramanujachary, K.M. Vijayakumar and C.S. Swamy, React. Kinet. Catal. Lett., 20 (1982) 233.
14 L. Wachowski, S. Zielinski and A. Sobczynski, Acta Chim. Hung., 113 (1983) 201.
15 R.F. Hicks and A.T. Bell, J. Catal., 91 (1985) 104.
16 R.P. Underwood and A.T. Bell, Appl. Catal., 34 (1987) 289.
17 P.R. Watson and G.A. Somorjai, J. Catal., 74 (1982) 282.
18 G.A. Somorjai and S.M. Davis, Chem. Technol., 13 (1983) 502.
19 J.R. Monnier and G. Apai, Div. Fuel Chem., Am. Chem. Soc., 31 (2) (1986) 239.
20 J.A. Broussard and L.E. Wade, Div. Fuel Chem., Am. Chem. Soc., 31 (3) (1986) 75.
21 H.J. Gysling, J.R. Monnier and G. Apai, J. Catal., 103 (1987) 407.
22 J.M.D. Tascón, S. Mendioroz and L.G. Tejuca, Z. Phys. Chem. N. F., 124 (1981) 109.
23 K. Ichimura, Y. Inoue and I. Yasumori, Bull. Chem. Soc. Jpn., 53 (1980) 3044.
24 N. Yamazoe, Y. Teraoka and T. Seiyama, Chem. Lett., (1981) 1767.
25 J.A. Marcos, R.H. Buitrago and E.A. Lombardo, J. Catal., 105 (1987) 95.
26 J.L.G. Fierro, M.A. Peña and L.G. Tejuca, J. Mater. Sci., 23 (1988) 1018.
27 L.G. Tejuca, A.T. Bell, J.L.G. Fierro and M.A. Peña, Appl. Surf. Sci., 31 (1988) 301.
28 S.J. Cochran and F.P. Larkins, J. Chem. Soc., Faraday Trans. 1, 81 (1985) 2179.
29 J.L.G. Fierro and L.G. Tejuca, J. Catal., 87 (1984) 126.
30 J.L.G. Fierro, J.M.D. Tascón and L.G. Tejuca, J. Catal., 89 (1984) 209.
31 J.M.D. Tascón, J.L.G. Fierro and L.G. Tejuca, J. Chem. Soc., Faraday Trans. 1, 81 (1985) 2399.
32 M. Crespin and W.K. Hall, J. Catal., 69 (1981) 359.
33 D.G. Blackmond and E.I. Ko, J. Catal., 96 (1985) 210.
34 G.B. Raupp and J.A. Dumesic, J. Phys. Chem., 89 (1985) 5240.
35 G. Busca and V. Lorenzelli, Mater. Chem., 7 (1982) 89.
36 L.G. Tejuca, C.H. Rochester, J.L.G. Fierro and J.M.D. Tascón, J. Chem. Soc., Faraday Trans. 1, 80 (1984) 1089.
37 R. Spinicci and A. Tofanari, React. Kinet. Catal. Lett., 27 (1985) 65.
38 J.M. Rynkowski, React. Kinet. Catal. Lett., 30 (1986) 41.
39 L.G. Tejuca, Thermochim. Acta, 126 (1988) 205.
40 E.G.M. Kuijpers, A.K. Breedijk, W.J.J. van der Wal and J.W. Geus, J. Catal., 81 (1983) 429.
41 E.G.M. Kuijpers, M.W.C.M.A. Nieuwesteeg, G.J. Wermer and J.W. Geus, J. Catal., 112 (1988) 107.
42 J.J. Prinsloo and P.C. Gravelle, J. Chem. Soc., Faraday Trans. 1, 76 (1980) 512.
43 R. Gopalakrishnan and B. Viswanathan, Surf. Technol., 23 (1984) 173.
44 V.C. Corberán, L.G. Tejuca and A.T. Bell, J. Mat. Sci., 1989, in press.
45 L.G. Tejuca, A.T. Bell, J.L.G. Fierro and J.M.D. Tascón, J. Chem. Soc., Faraday Trans. 1, 83 (1987) 3149.
46 M.P. Rosynek and D.T. Magnuson, J. Catal., 48 (1977) 417.